34th Annual International Conference of the IEEE EMBS
San Diego, California USA, 28 August - 1 September, 2012

# Effects of aging on thoracic aorta size and shape: A non-contrast CT study

Damian Craiem, Mariano E. Casciaro, Sebastian Graf, Gilles Chironi, Alain Simon and Ricardo L. Armentano

*Abstract*— **Measures of atherosclerosis burden like coronary artery calcification are performed using non-contrast heart CT. However, additional information can be derived from these studies, looking beyond the coronary arteries without exposing the patients to further radiation. We present a semi-automated method to assess ascending, arch and descending aorta geometry from non-contrast CT datasets in 250 normotensive patients. We investigated the effect of aging on thoracic aorta morphometry. The algorithm identifies the aortic centerline coordinates following a toroidal path for the curvilinear portion and axial planes for descending aorta. Then it reconstructs oblique planes orthogonal to the centerline direction and a circle fitting process estimates the vessel cross-section. Finally, global thoracic aorta dimensions (diameter, volume and length) and shape (vessel curvature and tortuosity, aortic arch width and height) are calculated. From a multivariate analysis, adjusted for gender and body-size area, aortic volume and arch width were the descriptors that better represented the aortic size and shape alterations with aging. The thoracic aorta suffers an expanding and unfolding process with aging that deserves further attention to prevent aortic aneurisms.**

## I. Introduction

The development of new screening tools for the detection of cardiovascular disease in its subclinical stage is needed. In clinical practice, coronary artery calcifications are assessed with non-contrast heart computed tomography (CT). Calcium score is a common measure of atherosclerotic disease burden, using a relative low radiation dose [1]. However, further information could be derived from these heartscans, looking beyond the coronary arteries. For example, additional anatomic information of the aorta could be obtained to early detect a pathologic enlargement that could terminate in ruptures or aneurisms.

In this work we propose to estimate the alterations of thoracic aorta (TA) size and shape with aging, taking advantage of non-contrast CT images. Aortic size is typically assessed with manual measurements of ascending and descending TA diameter, whereas the TA arch is commonly neglected [2, 3]. In fact, the complex geometry of the curvilinear part of the aorta may not be properly evaluated with planar estimations. In addition, there is no reason to limit aortic geometry assessment to 2D measurements when volumetric information is available with no additional cost. Several robust and complex aortic segmentation methods were developed in 3D and even 4D but they usually require contrast enhanced image modalities as CT and MRI angiography [4-6]. Segmentation algorithms in 3D that employ non-contrast CT images scarce and do not generally include the TA arch and were applied to a small number of subjects [7, 8].

The aim of this work is to identify the best size and shape descriptors of the aging effects on TA morphology in 3D. The TA geometry will be reconstructed from non-contrast cardiac CT scans with a custom software [9]. A population of 250 asymptomatic and normotensive patients will be studied. Descriptors of TA size and shape alterations with aging will be calculated and evaluated in multivariate models adjusted to gender and body-size area (BSA). Aortic changes per decade of life will be analyzed.

## II. Materials and Methods

A complete revision of the segmentation routine, centerline extraction and CSA estimation can be found in [9]. The population and CT scans are described in section A, the algorithms are explained in sections B and C. The entire process is sketched in Fig. 1.

### *A. Population and Image Acquisition*

We studied 250 normotensive patients from the CMPCV unit in the Pompidou Hospital (Paris, France). Subjects were asymptomatic and free of any overt cardiovascular disease. They had undergone non-contrast cardiac CT for CAC scoring in view of cardiovascular risk reclassification [1, 10]. The retrospective analysis of personal health data had the authorization of the CNIL (Commission nationale de l'informatique et des libertés) and was in accordance with the declaration of Helsinki. Images were obtained with a 64-slice MSCT scanner (Light-speed VCT; GE Health care, Milwaukee, Wisconsin, USA) using 2.5 mm slice thickness, 120 kVo, 250-mA tube current, 250-ms exposure time, a 2350-mm field of view and ECG triggering at the heart rate-dependent 60% percentage of the R-R interval (middle of diastole). Images were acquired in the craniocaudal direction from the top of the aortic arch to the level of the diaphragm in a single breath-hold. They were exported as DICOM files. The same reader imported these files and measured all the patients using the designed software presented in [9].

*Research supported by CONICET.

D.C, M.E.C., S.G. and R.L.A. are with the Favaloro University (Facultad de Ciencias Exactas y Naturales), Buenos Aires, Argentina (corresponding author to phone: +54 11 4378 1132; fax: +54 11 4384 0782; e-mail: dcraiem@ favaloro.edu.ar).

G.C. and A.S. are with the CMPCV unit of the HEGP Paris, France.

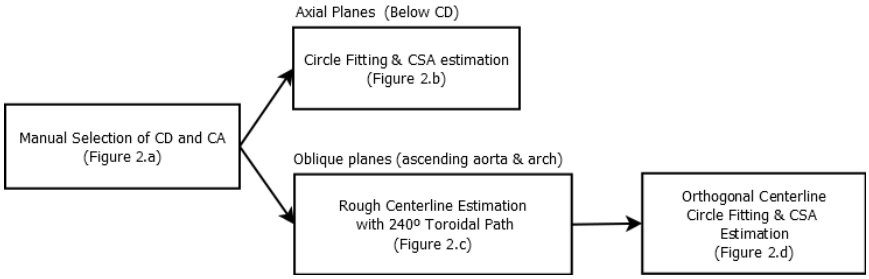


Figure 1. Centerline extraction and CSA estimation routine flowchart.

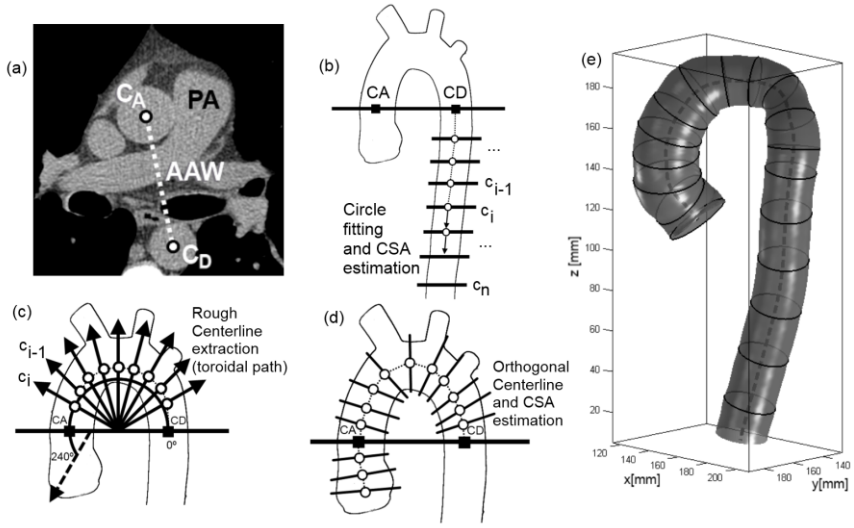


Figure 2. (a) $C_A$ (ascending) and $C_D$ (descending) seed-points at Pulmonary Artery (PA) level. White dotted-line represents aortic arch width (AAW). (b) Centerline extraction and CSA estimation scheme for axial planes below CD. (c) Rough Centerline extraction scheme, following a toroidal path of 240º connecting points CA and CD. (d) Orthogonal Centerline extraction and CSA estimation scheme, following the rough Centerline obtained in (c). (e) Aortic shape reconstruction. Dotted line represents the resulting Centerline and black circles represent (some) inscribed circles found in previous steps, connected by cylindrical surfaces.

### *B. Aortic Centerline Extraction*

The user selects the starting axial slice at the center of the pulmonary artery level and manually places 2 initial seed points inside the ascending and descending aorta cross-sections (Fig. 2.a). With the 2 seed points, an automated process extracts the TA centerline and estimates the vessel cross-sectional area (CSA) at each centerline coordinate relying on an adaptive circle-fitting algorithm that finds the largest circle inscribed into the vessel cross-section using planes orthogonal to the vessel centerline. This 4-steps circle-fitting algorithm starts automatically setting a 10x10 cm ROI where it performs:

- A 5x5 median filter that eliminates spurious noise.
- Morphological gray-scale opening transformation with a circle (r = 1 cm) as the structuring element.
- A k-means binarization (k=2) [11].
- An iterative circle growing sequence, where a small circle is placed on the seed point and iteratively expanded and displaced when its center when it touches a border.

Once the iterative process in the last step ends, the (x,y,z) coordinate of the circle center is considered as a valid point of the aortic centerline and its surface the corresponding CSA value. The circle-fitting algorithm is initially applied on the seed points placed by the user in the starting axial plane, to find the centerline points CA and CD (Fig. 2.a). First, axial images are analyzed below the descending aorta seed point CD (towards diaphragm) determining the centerline points $C_i$ of the descending aorta portion (Fig. 2.b under CD). For each successive plane i, the preceding $C_{i-1}$ circle center is used as the current seed point. After axial CSA estimation, all images above the descending aorta seed point CD (towards the annulus) are reformatted to reconstruct oblique planes following a torus sector (Fig. 2.c) through trilinear interpolation, to obtain a resolution of 0.5 mm (similar to axial resolution). For each successive oblique plane i, the previous $C_{i-1}$ circle center is used as the current seed point. The planes turn from angle 0º (seed point CD), passes through the top of the arch at 90º, then by the ascending seed point CA at 180º, until angle 240º at the annulus. At this stage, assuming axial planes for the descending portion of the aorta and oblique planes perpendicular to a 240º-toroid for its curvilinear path, the coordinates of the thoracic aorta midline are estimated. This discrete centerline coordinates are interpolated and smoothed using a 3D moving average filter to construct a rough approximation of the aortic centerline curve.

TABLE I. ABSOLUTE MORPHOMETRIC VALUES FOR AGE TERTILES (MEAN ± SD)

| Morphometric Descriptors | Age Tertiles | | |
|---|---|---|---|
| | *Young (39 - 51 y.o.)* | *Mid-Age (52 - 59 y.o.)* | *Old (60 - 73 y.o.)* |
| Diameter [cm] | 2.8 ± 0.2 | 2.9± 0.2 (+4%) † | 2.9 ± 0.2 (+6%) † |
| Length [cm] | 26.5 ± 2.2 | 27.8 ± 2.0 (+5%) † | 28.7 ± 3.1 (+8%) † |
| Volume [$cm^3$] | 132.1 ± 22.6 | 149.4 ± 30.8 (+13%) † | 162.0 ± 37.1 (+23%) † ‡ |
| Tortuosity | 0.88 ± 0.19 | 0.87±0.18 (-1%) | 0.86 ± 0.19 (-3%) |
| Curvature Radius [cm] | 3.0 ± 0.4 | 3.1 ± 0.4 (+6%) † | 3.2 ± 0.5 (+9%) † |
| Aortic Arch Width [cm] | 7.0 ± 0.7 | 7.6 ± 1.0 (+8%) † | 7.9 ± 1.0 (+12%) † |
| Aortic Arch Height [cm] | 5.1 ± 1.0 | 5.4 ± 1.2 (+6%) | 5.7 ± 1.2 (+11%) † |

†p<0.05 with respect to *Young*, ‡p<0.05 with respect to *Mid-Age* (Tukey-Kramer HSD post-hoc Test)

TABLE II. MULTIVARIATE ANALYSYS PER 10-YEARS ADJUSTED FOR GENDER AND BODY SIZE AREA

| Morphometric Descriptors | Model Parameters | | | | | | |
|---|---|---|---|---|---|---|---|
| | $\beta_{AGE}$ | *95% confidence interval* | $\beta_{SEX}$ | *95% confidence interval* | $\beta_{BSA}$ | *95% confidence interval* | *R* |
| Diameter [cm] | 0.14 | [0.11;0.17]‡ | -0.005 | [-0.040;0.03] | 0.5 | [0.36;0.64]‡ | 0.57 |
| Length [cm] | 1.6 | [1.12;2.0]‡ | 0.40 | [-0.05;0.84] | 2.4 | [0.64;4.22]† | 0.47 |
| Volume [$cm^3$] | 23.7 | [19.1;28.3]‡ | 3.0 | [-2.1;8.0] | 65.6 | [45.3;85.9]‡ | 0.61 |
| Tortuosity | -0.04 | [-0.1;-0.01]* | 0.002 | [-0.03;0.04] | -0.3 | [-0.4;-0.14]‡ | 0.30 |
| Curvature Radius [cm] | 0.2 | [0.18;0.3]‡ | 0.02 | [-0.05;0.09] | 1.0 | [0.8;1.3]‡ | 0.56 |
| Aortic Arch Width [cm] | 0.7 | [0.6;0.8]‡ | 0.13 | [-0.01;0.27] | 2.3 | [1.7;2.8]‡ | 0.65 |
| Aortic Arch Height [cm] | 0.4 | [0.3;0.6]‡ | 0.16 | [-0.05;0.36] | 1.0 | [0.1;1.8]* | 0.33 |

‡ p < 0.001; † p < 0.01; * p < 0.05

### C. CSA estimation

In this stage, orthogonal planes to the direction of the centerline curve extracted in section A are calculated for each centerline point. Within these oblique plane images, circles are inscribed for a second time, now resulting in roughly circular shapes in aortic cross-sectional planes (now more closely perpendicular to the centerline path). Each aortic centerline coordinate is now associated to its corresponding CSA value (Fig. 2.d).

For each patient, mean TA diameter, length and volume are calculated as size descriptors. The curvilinear part of the TA, from angles 0º to 240º, was described with the following shape descriptors: tortuosity, radius of curvature, aortic arch width (AAW) and height (AAH). Subjects were separated into three equicardinal groups divided by tertiles of the age distribution, and ANOVA was used to test differences in TA descriptors between them. Aging effects were analyzed in multivariate models adjusted for gender and BSA [3].

## III. RESULTS

We studied 200 men and 50 women (age 55 ± 7 y.o., age range 39 - 73): 77% were hypercholesterolemic, 26% smokers and 5% diabetics. Mean systolic and diastolic blood pressures were 119±10 mmHg and 71±8 mmHg respectively.

Aortic size and shape descriptors are shown in Table I for patients separated by age tertiles in three groups (Young, Mid-Age and Old). ANOVA showed that aortic size increased and aortic arch unfolded with age (p<0.001 for all descriptors except p<0.01 for AAH). The strongest association was found with aortic volume (+23% from young to older subjects).

In multivariate analysis, adjusted for male gender and BSA (Table II), all aortic size and shape descriptors increased with age (p<0.001), except tortuosity that decreased (p<0.05). It is to note that age, male gender and BSA jointly accounted for 61% and 65% of the variability in aortic volume and aortic arch width (AAW) models, respectively.

## IV. DISCUSSION

The main findings of this work are that TA volume was better than diameter and length to evaluate changes in TA size with aging. Furthermore, the AAW was a remarkable descriptor to explain the vessel unfolding alteration.

The studies that evaluate the TA size using non-contrast CT measure mostly diameters, adjusted for age and BSA [2, 3, 10]. The reconstruction of the TA in 3D using non-contrast CT images is not frequent [7, 8] and most of the reports choose contrast CT or MRI techniques [4-6, 12].The main advantage of using non-contrast CT images is that they can be simultaneously employed for calcium score determinations that are primarily intended for coronary artery calcium measurement in cardiovascular risk refinement [10, 13]. Overall, our technique is fast (a few minutes) and brings new TA size and shape information that can be used to early predict aneurism before dissection or rupture [14]. All this features makes our approach acceptable for clinical practice.

When patients were divided in age tertiles, TA volume was better than diameter and length to evidence the TA size alterations with aging (Table I). Probably, because TA volume integrates the vessel radial expansion and lengthening. In the multivariate model, adjusted for age and BSA, diameter and length increased 1.4 mm and 16 mm every decade of life, respectively (Table 2). Wolak et al. found similar values for diameter in more than 4000 patients, with values per decade of life of 1.3 mm for ascending and 1.1 mm for descending TA. Lengthening is more difficult to assess and depends on the definition of the vessel segments. Sugawara et al. reported that the aorta lengthens 12% per decade of life due primarily to the elongation of the ascending aorta [15]. This percentage is somehow higher than the 5-8% found in our study but reasonable with respect to the 4-6% increase in cross-sectional expansion reported here (Table 1) and elsewhere [16]. Again, probably the exact definition of the start and end of the TA is critical due to vessel tethering.

The TA shape alterations with aging showed an unfolding process that included a decrease in tortuosity and an increase in radius of curvature for the arch. This curvilinear part of the vessel simultaneously increased its size and uncoiled with aging [9, 12, 17]. In a multivariate model AAW was the descriptor that better reflected these alterations and could explain more than 65% of the model variability (Table II). For clinical purposes, the AAW can be estimated from a single axial plane measuring the distance between the ascending and descending TA centers and could be proposed as a simple marker of aortic unfolding and geometric transformation with age.

In multivariate analysis, $\beta_{SEX}$ parameter showed no significant relation with the change in size or shape descriptors, suggesting that females are subject to the same TA geometric transformations with age than male subjects. Nonetheless, the higher prevalence of men than women in our study limits the extrapolation to the general population.

In relation to other vessel segmentation methods the proposed algorithm can be seen as a centerline + cross-sectional model [18], where cross sections are strictly circular and a reliable centerline estimation can be obtained due to its regularity along aortic pathway. In contrast to other similar models, the proposed adaptive growing circle works even in low-contrast structures but relies not only on axial planes, depending on the reconstruction of oblique planes that approximates aortic pathway for its curvilinear portion as a toroidal path.

Our study has two main limitations. First, the TA size includes the vessel wall due to the lack of contrast. Second, the proposed method is semiautomatic and requires manual intervention in the selection of ascending and descending aorta cross -sections at pulmonary artery bifurcation level. The former is inherent to the CT technique and the latter should be improved with automatic landmarks detection (e.g. pulmonary artery centerline at its bifurcation level).

## ACKNOWLEDGMENT

The authors want to thank Dr. Elie Mousseaux and Dr. Alban Redheuil for their important contribution.

## REFERENCES

[1] A. Simon, G. Chironi, and J. Levenson, "Comparative performance of subclinical atherosclerosis tests in predicting coronary heart disease in asymptomatic individuals," *Eur Heart J,* vol. 28, no. 24, pp. 2967-71, 2007.

[2] Y. Agmon, B. K. Khandheria, I. Meissner *et al.*, "Is aortic dilatation an atherosclerosis-related process? Clinical, laboratory, and transesophageal echocardiographic correlates of thoracic aortic dimensions in the population with implications for thoracic aortic aneurysm formation," *J Am Coll Cardiol,* vol. 42, no. 6, pp. 1076-83, 2003.

[3] A. Wolak, H. Gransar, L. E. J. Thomson *et al.*, "Aortic size assessment by noncontrast cardiac computed tomography: Normal limits by age, gender, and body surface area," *JACC: Cardiovascular Imaging,* vol. 1, no. 2, pp. 200-209, 2008.

[4] T. Behrens, K. Rohr, and H. S. Stiehl, "Robust segmentation of tubular structures in 3-d medical images by parametric object detection and tracking," *IEEE Trans Syst Man Cybern B Cybern,* vol. 33, no. 4, pp. 554-61, 2003.

[5] S. Worz, H. von Tengg-Kobligk, V. Henninger *et al.*, "3-d quantification of the aortic arch morphology in 3-d cta data for endovascular aortic repair," *IEEE Trans Biomed Eng,* vol. 57, no. 10, pp. 2359-68, 2010.

[6] F. Zhao, H. Zhang, A. Wahle *et al.*, "Congenital aortic disease: 4d magnetic resonance segmentation and quantitative analysis," *Med Image Anal,* vol. 13, no. 3, pp. 483-93, 2009.

[7] T. Kovács, "Automatic segmentation of the vessel lumen from 3d cta images of aortic dissection.," *Selected readings in vision and graphics*, 65, G. S. Luc Van Gool, Markus Gross, Bernt Schiele, ed., Konstanz, Germany, 2010.

[8] U. Kurkure, O. C. Avila-Montes, and I. A. Kakadiaris, "Automated segmentation of thoracic aorta in non-contrast ct images." pp. 29-32.

[9] D. Craiem, G. Chironi, A. Redheuil *et al.*, "Aging impact on thoracic aorta 3d morphometry in intermediate-risk subjects: Looking beyond coronary arteries with non-contrast cardiac ct," *Annals of Biomedical Engineering*, pp. 1-11, 2011.

[10] G. Chironi, L. Orobinskaia, J. L. Megnien *et al.*, "Early thoracic aorta enlargement in asymptomatic individuals at risk for cardiovascular disease: Determinant factors and clinical implication," *J Hypertens,* vol. 28, no. 10, pp. 2134-8, 2010.

[11] T. Kanungo, D. M. Mount, N. S. Netanyahu *et al.*, "An efficient k-means clustering algorithm: Analysis and implementation," *IEEE Trans. Pattern Anal. Mach. Intell.,* vol. 24, no. 7, pp. 881-892, 2002.

[12] A. Redheuil, W. C. Yu, E. Mousseaux *et al.*, "Age-related changes in aortic arch geometry: Relationship with proximal aortic function and left ventricular mass and remodeling," *Journal of the American College of Cardiology,* vol. 58, no. 12, pp. 1262-1270, 2011.

[13] P. Greenland, J. S. Alpert, G. A. Beller *et al.*, "2010 accf/aha guideline for assessment of cardiovascular risk in asymptomatic adults: A report of the american college of cardiology foundation/american heart association task force on practice guidelines," *J Am Coll Cardiol,* vol. 56, no. 25, pp. e50-103, 2010.

[14] J. A. Elefteriades, and E. A. Farkas, "Thoracic aortic aneurysm clinically pertinent controversies and uncertainties," *J Am Coll Cardiol,* vol. 55, no. 9, pp. 841-57, 2010.

[15] J. Sugawara, K. Hayashi, T. Yokoi *et al.*, "Age-associated elongation of the ascending aorta in adults," *J Am Coll Cardiol Img,* vol. 1, no. 6, pp. 739-748, 2008.

[16] R. S. Vasan, M. G. Larson, and D. Levy, "Determinants of echocardiographic aortic root size. The framingham heart study," *Circulation,* vol. 91, no. 3, pp. 734-40, 1995.

[17] M. O'Rourke, A. Farnsworth, and J. O'Rourke, "Aortic dimensions and stiffness in normal adults," *JACC Cardiovasc Imaging,* vol. 1, no. 6, pp. 749-51, 2008.

[18] D. Lesage, E. D. Angelini, I. Bloch *et al.*, "A review of 3d vessel lumen segmentation techniques: Models, features and extraction schemes," *Med Image Anal,* vol. 13, no. 6, pp. 819-45, 2009.